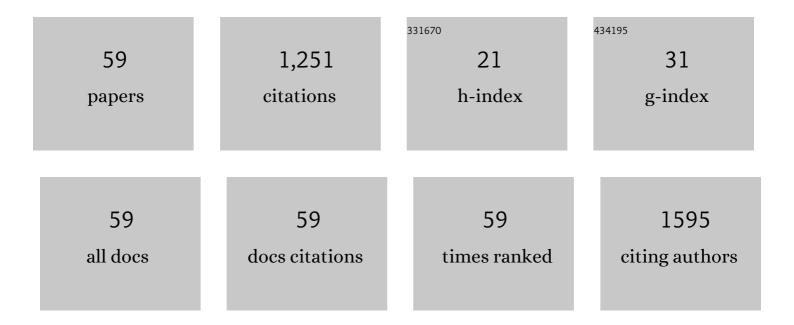
## Jingxia Yang

List of Publications by Year in descending order

Source: https://exaly.com/author-pdf/6984054/publications.pdf

Version: 2024-02-01



ΙΝΟΧΙΑ ΥΛΝΟ

#	Article	IF	CITATIONS
1	CeO2 Structure Adjustment by H2O via the Microwave–Ultrasonic Method and Its Application in Imine Catalysis. Frontiers in Chemistry, 2022, 10, .	3.6	1
2	Differential Sensing of Antibiotics Using Metal Ions and Gold Nanoclusters Based on TMB–H2O2 System. Chemosensors, 2022, 10, 222.	3.6	1
3	Nitrate Precursor Driven High Performance Ni/Co-MOF Nanosheets for Supercapacitors. ACS Applied Nano Materials, 2022, 5, 8382-8392.	5.0	23
4	Microwave-aided synthesis of BiOI/g-C3N4 composites and their enhanced catalytic activities for Cr(VI) removal. Chemical Physics Letters, 2021, 762, 138143.	2.6	26
5	B-Doped g-C <sub>3</sub> N <sub>4</sub> Quantum Dots-Modified Ni(OH) <sub>2</sub> Nanoflowers as an Efficient and Stable Electrode for Supercapacitors. ACS Applied Energy Materials, 2021, 4, 1496-1504.	5.1	19
6	A stable super-amphiphilic surface created from superhydrophobic silica/epoxy coating by low-temperature plasma-treatment. Surface Engineering, 2021, 37, 1282-1289.	2.2	5
7	Highly Enhanced Visibleâ€light Photocatalytic Activity via a Novel Surface Structure of CeO <sub>2</sub> /gâ^2C <sub>3</sub> N <sub>4</sub> toward Removal of 2,4â€dichlorophenol and Cr(VI). ChemCatChem, 2021, 13, 2034-2044.	3.7	14
8	Enhanced interface properties of solution-processed antimony sulfide planar solar cells with n-type indium sulfide buffer layer. Electrochimica Acta, 2021, 376, 138031.	5.2	17
9	Co <sub>3</sub> O <sub>4</sub> â^'CeO <sub>2</sub> Nanocomposites for Lowâ€Temperature CO Oxidation. Chemistry - A European Journal, 2021, 27, 16947-16955.	3.3	15
10	Grain Size and Interface Modification via Cesium Carbonate Post-Treatment for Efficient SnO <sub>2</sub> -Based Planar Perovskite Solar Cells. ACS Applied Energy Materials, 2021, 4, 7002-7011.	5.1	32
11	Copper (II) Ion-Modified Gold Nanoclusters as Peroxidase Mimetics for the Colorimetric Detection of Pyrophosphate. Sensors, 2021, 21, 5538.	3.8	12
12	One-pot solvothermal synthesis of CoNi2S4/reduced graphene oxide (rGO) nanocomposites as anode for sodium-ion batteries. Ionics, 2020, 26, 213-221.	2.4	9
13	Structure design of CeO2–MoS2 composites and their efficient activity for imine synthesis. Applied Nanoscience (Switzerland), 2020, 10, 233-241.	3.1	9
14	Spray-coated monodispersed SnO2 microsphere films as scaffold layers for efficient mesoscopic perovskite solar cells. Journal of Power Sources, 2020, 448, 227405.	7.8	58
15	Fabrication of hierarchical MnxOy@SiO2@C-Ni nanowires for enhanced catalytic performance. Colloids and Surfaces A: Physicochemical and Engineering Aspects, 2020, 586, 124211.	4.7	7
16	Anatase TiO2 nanorod arrays as high-performance electron transport layers for perovskite solar cells. Journal of Alloys and Compounds, 2020, 849, 156629.	5.5	25
17	Energy-Guided Shape Control Towards Highly Active CeO2. Topics in Catalysis, 2020, 63, 1743-1753.	2.8	9
18	Shapeâ€Dependent CeO <sub>2</sub> @BiOI for Degradation of Aqueous Cr(VI). Advanced Materials Interfaces. 2020. 7. 1901879.	3.7	23

Jingxia Yang

#	Article	IF	CITATIONS
19	Black SnO <sub>2</sub> –TiO <sub>2</sub> Nanocomposites with High Dispersion for Photocatalytic and Photovoltalic Applications. ACS Applied Nano Materials, 2020, 3, 4265-4273.	5.0	33
20	Large CeO2 nanoflakes modified by graphene as barriers in waterborne acrylic coatings and the improved anticorrosion performance. Progress in Organic Coatings, 2020, 143, 105607.	3.9	20
21	Solution-processed p-type nanocrystalline CoO films for inverted mixed perovskite solar cells. Journal of Colloid and Interface Science, 2020, 573, 78-86.	9.4	19
22	Fast visual evaluation of the catalytic activity of CeO2: Simple colorimetric assay using 3,3′,5,5′-tetramethylbenzidine as indicator. Journal of Catalysis, 2020, 389, 71-77.	6.2	17
23	Enhanced Corrosion Resistance of Silicone-Modified Epoxy Coatings by Surface-Wave Plasma Treatment. International Journal of Electrochemical Science, 2019, , 5051-5063.	1.3	2
24	Anchoring nickel nanoparticles on three-dimensionally macro-/mesoporous titanium dioxide with a carbon layer from polydopamine using polymethylmethacrylate microspheres as sacrificial templates. Materials Chemistry Frontiers, 2019, 3, 224-232.	5.9	62
25	Cysteine-rich protein-templated silver nanoclusters as a fluorometric probe for mercury( <scp>ii</scp> ) detection. Analytical Methods, 2019, 11, 733-738.	2.7	13
26	BiSbS3@N-doped carbon core–shell nanorods as efficient anode materials for sodium-ion batteries. Dalton Transactions, 2019, 48, 10448-10454.	3.3	22
27	Plasma treated h-BN nanoflakes as barriers to enhance anticorrosion of acrylic coating on steel. Progress in Organic Coatings, 2019, 133, 139-144.	3.9	28
28	Copper(II) ions enhance the peroxidase-like activity and stability of keratin-capped gold nanoclusters for the colorimetric detection of glucose. Mikrochimica Acta, 2019, 186, 271.	5.0	32
29	Template-free synthesis of hierarchical NiO microtubes as high performance anode materials for Li-ion batteries. Current Applied Physics, 2019, 19, 715-720.	2.4	10
30	Monodispersed SnO2 microspheres aggregated by tunable building units as effective photoelectrodes in solar cells. Applied Surface Science, 2019, 463, 679-685.	6.1	19
31	Fluorescence enhancement of cysteine-rich protein-templated gold nanoclusters using silver(I) ions and its sensing application for mercury(II). Sensors and Actuators B: Chemical, 2018, 267, 342-350.	7.8	61
32	Surface modification of CeO2 nanoflakes by low temperature plasma treatment to enhance imine yield: Influences of different plasma atmospheres. Applied Surface Science, 2018, 454, 173-180.	6.1	27
33	Large Dimensional CeO <sub>2</sub> Nanoflakes by Microwaveâ€Assisted Synthesis: Lamellar Nanoâ€Channels and Surface Oxygen Vacancies Promote Catalytic Activity. ChemCatChem, 2018, 10, 4100-4108.	3.7	29
34	RGO modified ZnAl-LDH as epoxy nanostructure filler: A novel synthetic approach to anticorrosive waterborne coating. Surface and Coatings Technology, 2017, 326, 207-215.	4.8	72
35	Surface oxygen vacancies dominated CeO2 as efficient catalyst for imine synthesis: Influences of different cerium precursors. Molecular Catalysis, 2017, 443, 131-138.	2.0	32
36	In situ formation of reduced graphene oxide structures in ceria by combined sol–gel and solvothermal processing. Beilstein Journal of Nanotechnology, 2016, 7, 1815-1821.	2.8	11

JINGXIA YANG

#	Article	IF	CITATIONS
37	Different Synthesis Protocols for Co <sub>3</sub> O <sub>4</sub> –CeO <sub>2</sub> Catalysts—Partâ€1: Influence on the Morphology on the Nanoscale. Chemistry - A European Journal, 2015, 21, 885-892.	3.3	24
38	High Surface Area Ceria for CO Oxidation Prepared from Cerium t-Butoxide by Combined Sol–Gel and Solvothermal Processing. Catalysis Letters, 2014, 144, 403-412.	2.6	40
39	Sol-gel Synthesis and Photoluminescence Characterization of Ba <sub>2</sub> SiO <sub>4</sub> :Eu <sup>2+</sup> Green Phosphors for White-LED Application. Integrated Ferroelectrics, 2014, 154, 128-134.	0.7	14
40	Enhanced Sunlight Photocatalytic Performance of Hafnium Doped ZnO Nanoparticles for Methylene Blue Degradation. Integrated Ferroelectrics, 2013, 145, 108-114.	0.7	14
41	Tuning the Band Gap of Stable and Dispersible Graphene Aqueous Solution via Hydrothermal Reduction Method. Integrated Ferroelectrics, 2013, 145, 115-121.	0.7	1
42	Solvothermal Preparation of Carbon-Enhanced TiO2/Graphene Composite and Its Visible Light Photocatalytic Properties. Integrated Ferroelectrics, 2012, 138, 152-158.	0.7	6
43	Influence of anionic concentration and deposition temperature on formation of wurtzite CdS thin films by in situ chemical reaction method. Journal of Alloys and Compounds, 2012, 517, 54-60.	5.5	11
44	Zinc(II) Complexes with Dangling Functional Organic Groups. European Journal of Inorganic Chemistry, 2012, 2012, 4294-4300.	2.0	12
45	Sol–gel synthesis of ZnTiO3 using a single-source precursor based on p-carboxybenzaldehyde oxime as a linker. Journal of Materials Chemistry, 2012, 22, 24034.	6.7	18
46	Green synthesis by diethylene glycol based solution process and characterization of SnS nanoparticles. Crystal Research and Technology, 2012, 47, 461-466.	1.3	11
47	Multi‣ayer Deposition and Characteristics of Nanocrystal <scp><ds< scp=""></ds<></scp> Thin Films by an <i>In situ</i> Chemical Reaction Process. Journal of the American Ceramic Society, 2012, 95, 3037-3042.	3.8	4
48	Controllable synthesis of hexagonal and orthorhombic YFeO3 and their visible-light photocatalytic activities. Materials Letters, 2012, 81, 1-4.	2.6	81
49	An in-situ chemical reaction deposition of nanosized wurtzite CdS thin films. Thin Solid Films, 2012, 520, 1826-1831.	1.8	20
50	Preparations of TiO2 nanocrystal coating layers with various morphologies on Mullite fibers for infrared opacifier application. Thin Solid Films, 2012, 520, 2651-2655.	1.8	13
51	Preparation and characterization of SnS nanocrystals by a triethanolamine-assisted diethylene glycol solution synthesis. Applied Surface Science, 2011, 258, 1353-1358.	6.1	22
52	Preparation and characteristics of CdS thin films by dip-coating method using its nanocrystal ink. Materials Letters, 2011, 65, 1340-1343.	2.6	12
53	Preparation of mesoporous titania by surfactant-assisted sol–gel processing of acetaldoxime-modified titanium alkoxides. Journal of Non-Crystalline Solids, 2010, 356, 1217-1227.	3.1	30
54	Electrodeposition of CuInSe2 films by an alternating double-potentiostatic method using nearly neurly neutral electrolytes. Electrochemistry Communications, 2009, 11, 711-714.	4.7	22

JINGXIA YANG

#	Article	IF	CITATIONS
55	Growth and characterization of CulnSe2 thin films prepared by successive ionic layer adsorption and reaction method with different deposition temperatures. Thin Solid Films, 2009, 517, 6617-6622.	1.8	15
56	Kinetic Growth of One-Dimensional Zinc-Blende CdTe Nanocrystals by Aqueous Synthesis at Low Temperature. Crystal Growth and Design, 2009, 9, 5077-5082.	3.0	11
57	An investigation into effect of cationic precursor solutions on formation of CulnSe2 thin films by SILAR method. Solar Energy Materials and Solar Cells, 2008, 92, 621-627.	6.2	31
58	Preparation and Process Chemistry of SnO2Films Derived from SnC2O4by the Aqueous Sol–Gel Method. Journal of the American Ceramic Society, 2008, 91, 1939-1944.	3.8	15
59	Formation of rod-crystals on CuInSe2 thin films by SILAR method using CH3–(CH2)11–C6H4–SO3Na surfactant. Materials Letters, 2008, 62, 4177-4180.	2.6	10